

Article

Raman Assisted Fiber Optical Parametric Amplifier for S-Band Multichannel Transmission System

Andis Supe ¹, Kaspars Zakis ¹, Lilita Gegere ¹, Dmitrii Redka ^{1,2}, Jurgis Porins ¹, Sandis Spolitis ¹
and Vjaceslavs Bobrovs ^{1,*}

¹ Institute of Telecommunications, Riga Technical University, Azenes st. 12, LV-1048 Riga, Latvia; andis.supe@rtu.lv (A.S.); kaspars.zakis@rtu.lv (K.Z.); lilita.gegere@rtu.lv (L.G.); dnredka@etu.ru (D.R.); jurgis.porins@rtu.lv (J.P.); sandis.spolitis@rtu.lv (S.S.)

² Department of Photonics, Electrotechnical University “LETI” (ETU), 5 Prof. Popova Street, 197376 Saint Petersburg, Russia

* Correspondence: vjaceslavs.bobrovs@rtu.lv

Abstract: In this paper we present results from the study of optical signal amplification using Raman assisted fiber optical parametric amplifier with considerable benefits for S-band telecommunication systems where the use of widely used erbium-doped fiber amplifier is limited. We have created detailed models and performed computer simulations of combined Raman and fiber optical parametric amplification in a 16-channel 40 Gbps/channel wavelength division multiplexed transmission system. Achieved gain bandwidth, as well as transmission system parameters—signal-to-noise ratio and bit-error-ratio—were analyzed by comparing the Raman assisted fiber optical parametric amplifier to the single pump fiber optical parametric amplifier. Results show that the 3 dB gain bandwidth in the case of combined amplification is up to 0.2 THz wider with 1.9 dB difference between the lowest and highest gain.

Keywords: optical amplifiers; fiber nonlinear optics; fiber optical transmission system; wavelength division multiplexing



Citation: Supe, A.; Zakis, K.; Gegere, L.; Redka, D.; Porins, J.; Spolitis, S.; Bobrovs, V. Raman Assisted Fiber Optical Parametric Amplifier for S-Band Multichannel Transmission System. *Fibers* **2021**, *9*, 9. <https://doi.org/10.3390/fib9020009>

Received: 30 November 2020

Accepted: 15 January 2021

Published: 01 February 2021

Publisher's Note: MDPI stays neutral with regard to jurisdictional claims in published maps and institutional affiliations.



Copyright: © 2021 by the authors. Licensee MDPI, Basel, Switzerland. This article is an open access article distributed under the terms and conditions of the Creative Commons Attribution (CC BY) license (<https://creativecommons.org/licenses/by/4.0/>).

1. Introduction

The development of optical transmission systems is mainly determined by the demand for a steadily increasing amount of data to be transmitted over telecommunications networks. Moreover, forecasts indicate that this process will continue. Company Cisco predicts that overall Internet Protocol (IP) traffic will grow at a compound annual growth rate (CAGR) of 26% from 2017 to 2022 [1]. Despite the rapid development of mobile communication systems fiber optics still have a major role in backhaul and access networks. According to the Ericsson Mobility Report, around half of all households in the world, i.e., over 1 billion—are yet to have a fixed broadband connection [2]. A large amount of data transmission requires high-speed transmission systems. One of such technologies that can offer information broadcast at high data rates is optical transmission systems based on wavelength division multiplexing (WDM).

WDM technologies were developed already in the mid-1990s and allowed parallel transmission of several WDM channels on the same fiber [3]. The first systems were so-called coarse WDM (CWDM) with an interchannel band of ~20 nm. The development of more stable laser sources and improvements in optical filtering allowed closer channel allocation thus introducing dense WDM (DWDM) systems with significantly higher spectral effectivity compared to CWDM. The total fiber capacity evolution using WDM is ensured mainly by the steady increase in the bandwidth of optical amplifiers as well as the increase in spectral efficiency due to improvements in transmitter and receiver components.

The fiber bandwidth that is considered usable for long-distance transmission occupies the wavelength range from ~1300 to ~1700 nm, where typical standard single mode fiber

(SSMF) loss is moderate or low (≤ 0.35 dB/km). This corresponds to a full channel bandwidth of 54 THz [3], which is divided into smaller sub-bands. In practical implementations, the usable bandwidth for long reach transmission is limited by the gain bandwidth of applied amplification technology. In the case of widely used erbium-doped fiber amplifier (EDFA), the gain bandwidth covers only C (1530–1565 nm) and partly L (1565–1625 nm) bands (5–10 THz). To overcome this limitation, multiple amplification technologies can be used in parallel to form multiband amplifiers and transmission systems [4–9].

When talking about combined amplification the first option with which it is associated is Raman-EDFA combined amplifier. EDFA amplifiers are widely used in existing fiber optics transmission systems due to their relatively low price and sufficiently large gain (up to 30 dB and higher) [10]. Raman-EDFA combination allows smoothing out the EDFA gain spectrum which is quite uneven and is hard to be equalized using only EDFA pumping lasers [11]. Hybrid Raman-EDFAs also can achieve effective noise figures typically 3 to 6 dB better than can be achieved with an EDFA alone. Fiber Raman amplifier (FRA) effective noise figure is in the range of less than zero dB almost down to -2 dB. That is possible because the effective noise figure is defined as the noise figure of the hypothetical (nonphysical) discrete amplifier which if placed at the output of the span would provide the same gain and noise level as the distributed Raman amplifier [12]. The main drawback of hybrid Raman-EDFA is still limited EDFA gain bandwidth overlapping with C, L bands. Therefore, this combination only improves EDFA characteristics but does not give any additional flexibility concerning wavelength. It should be noted that the wavelength band can be extended towards S-band (1460–1530 nm) using Thulium doped fiber amplifiers [13–15]. However, these amplifiers are less efficient since amplification is based on a four-level transition and require the use of fluoride glass as host medium [16]. Therefore, more promising solutions are amplifiers which gain bandwidth can be modified by using appropriate pump lasers, for example, Raman and fiber optical parametric amplifiers.

The advantage of FRAs is the possibility to adjust the gain curve frequency band by selecting a pump laser wavelength [17]. Raman amplification is a relatively broadband effect, having gain bandwidth >5 THz [18] with the possibility to widen it and engineer its profile using multiple pump lasers [19]. The main drawback of the FRAs is relatively low pumping efficiency in the case of weak input signals. This means that a powerful pump laser is required to achieve the necessary signal gain because more than 30% of pump power is wasted [20,21]. Therefore, Raman amplifiers require pump powers in the range of 1 to 5 W. If compared to EDFA the pump power is almost two orders of magnitude higher to achieve the same level of gain [18]. One more disadvantage is the fast gain response time that causes noise generation.

Another very promising amplification technique is fiber optical parametric amplifiers (FOPA) based on a nonlinear optical effect—four-wave mixing (FWM). FOPA gain bandwidth and position in the frequency range is very similar to FRAs. Gain characteristics can be modified by selecting the appropriate pump laser and the provided gain is more efficient compared to Raman amplification [22]. Idler components that are generated during FWM can also be used for wavelength conversion. To realize FOPA it is necessary to ensure phase matching between pump laser and signals to be amplified to achieve effective signal amplification. Phase matching depends on lots of aspects including pump and signal wavelength, power, fiber dispersion, nonlinear characteristics [23–28]. The flatness and symmetry of the resulting gain profile can also be limited by the Raman effect [29]. FOPAs with gain as high as 70 dB and bandwidth ≥ 200 nm have been implemented under laboratory conditions [30,31]. One of the main FOPA drawbacks in WDM systems is the undesired FWM interaction between signals that are amplified in a nonlinear environment leading to inter-channel crosstalk [32–34]. FOPA performance can be improved with more complex setups that include the use of a bi-directional looped architecture, multi-section gain media, or splitting of the signal into two orthogonal polarizations to enable polarization-insensitive signal gain [33,35–40].

A very promising approach for mitigating FRA and FOPA drawbacks is hybrid amplification methods that have been extensively studied for various applications [5,8,31,41–49]. This combination is the Raman assisted FOPA (RA-FOPA) amplifier. The main idea is that the FOPA amplifier is supplemented with a Raman pump connected in the backward direction [45]. Thus, in the same fiber two nonlinear effects are involved in the signal amplification: Stimulated Raman scattering and four-wave mixing. The gain behavior of RA-FOPAs is rather complex. The overall gain can be larger than the sum of the individual gain of Raman and parametric amplifiers [45–47].

Raman pump wavelength typically is set in such a way to amplify the parametric pump laser since the Raman scattering effect is more efficient for higher power optical component amplification. The Raman pump power transmission to the signal mostly occurs indirectly through the parametric pump. However, part of signal gain also occurs directly through the Raman amplification process [47]. Backward Raman pumping scheme is more suitable for RA-FOPA amplifier to suppress the signal power fluctuation caused by parametric pump relative intensity noise [50] as well as to mitigate undesirable Raman pump to parametric pump interaction through the FWM process in a nonlinear medium, for example, highly nonlinear fiber (HNLF).

RA-FOPA amplifiers have been studied for various purposes. Firstly the basic idea has been tested and described in several publications where the principles and benefits of this combination were analyzed [5,8,31,41–45,47,48]. In these publications, the focus is on the combined amplifier gain spectra as well as the efficiency of different pumping schemes and noise figures. However, in the more recent publications, the use of RA-FOPA in the WDM systems have been studied analytically [51] and experimentally [49]. In the latter mentioned publication, the RA-FOPA performance was studied in the case of 10 channel WDM system working in the C band with per-channel signal power at the amplifier input up to -20 dBm.

In this paper, we show results from the analysis of potential use of RA-FOPA amplifier in 16 channel WDM system operating in the optical S-band with 100 GHz channel spacing. Amplifier input signal power per channel was set to be -40 dBm that has a good match with long haul transmission systems or passive optical networks with a large degree of branching like metro or access networks. The main goal of this research is to find the RA-FOPA configuration that makes possible very weak optical signal amplification in the S optical band while minimizing power difference among all the WDM system channels. The proposed RA-FOPA setup will be compared to a single pump FOPA amplifier with the same maximum output signal power level to evaluate performance improvements due to the addition of a FRA.

The research of RA-FOPA is based on computer simulations performed by Synopsis OptSim software implementing field-proven split-step method to solve the non-linear Schrodinger equation [52]. Optical amplifier performance was evaluated by analyzing gain curves and estimating power penalty according to received signal power as well as received optical signal to noise ratio (OSNR) and bit error ratio (BER).

This paper consists of four sections. First of all, there is an explanation of the proposed amplifier simulation scheme. The second section covers simulations' results for single pump FOPA and RA-FOPA setups. The third section is dedicated to the analysis of simulations' results. The final chapter contains the summary and conclusions of this research.

2. The Architecture of the RA-FOPA Hybrid Amplifier Simulation Scheme

In this section of the paper, the simulation scheme of the RA-FOPA hybrid amplifier is described. The simulation setup (Figure 1) consists of four main sections: transmitters (Tx), transmission line, RA-FOPA amplifier, and receivers (Rx). The transmitter section consists of 16 transmitters with a typical construction composed of a 40 Gbps pseudo-random bit pattern generator that is connected to a non-return to zero (NRZ) coder that drives a Mach-Zehnder modulator (MZM). MZM optical input is connected to the light source

(in this case distributed feedback laser—DFB). Consequently, all sources are generating 40 Gbps NRZ coded on-off keying (NRZ-OOK) optical signals. The only difference between all the transmitters is that each of them has its unique carrier frequency spaced by 100 GHz, occupying the S-band frequencies from 196.1 THz to 197.6 THz (1517.168 nm to 1528.773 nm).

Respectively, all 16 NZR-OOK transmitters are anchored in the optical S-band (1460–1530 nm) that is out of the commonly used EDFA amplification range. Next, all the 16 channels are multiplexed together using an optical coupler and then transmitted through 150 km of either a standard SMF (ITU-T G.652) or NZ-DSF (ITU-T G.655) fiber, the key parameters of which at a reference wavelength of 1550 nm are shown in Table 1, which also contains data about the HNLF used in the amplifier section.

Table 1. Fiber parameters used for the transmission line.

Parameter	Fiber Type		
	Standard SMF	NZ-DSF	HNLF
Attenuation coefficient (dB/km)	0.20	0.19	0.96
Dispersion coefficient (ps/nm/km)	18	4	0
Dispersion slope (ps/(nm ² km))	0.086	0.108	0.016
Effective area (μm ²)	85	72	10
Nonlinear index (m ² /W)	2.21×10^{-20}	2.31×10^{-20}	3.7×10^{-20}

As per-channel power of −40 dBm is too low to be received by using a PIN photodiode at an acceptable BER, it requires preamplification. Due to technology maturity, a typical solution for WDM systems is EDFA based preamplifier which allows it to improve the receiver sensitivity up to −38.8 dBm at 40 Gbps [53,54]. However, FOPA can provide even higher sensitivity as described in various papers [54,55]. Therefore, in this research, we have studied the RA-FOPA performance in the case of weak signal amplification. As one can see in Figure 1, after the coupler, there is an isolator to block reflected signals from entering transmitters.

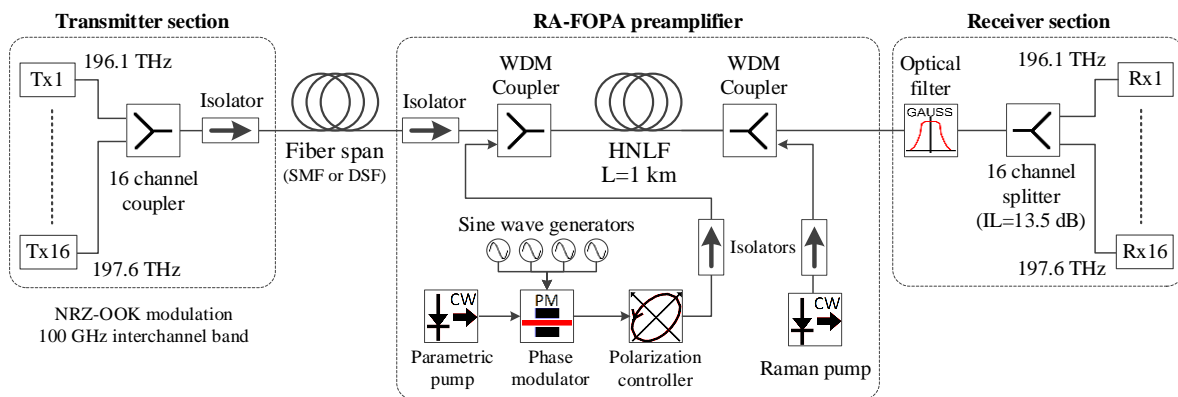


Figure 1. Simulation scheme of Raman assisted fiber optical parametric amplifiers (RA-FOPA) preamplifier in the 16-channel wavelength division multiplexing (WDM) system.

Based on previous work in [56] the RA-FOPA amplifier consists of a parametric pump (PP) that is a CW laser emitting at 1553.99 nm (192.918 THz) and output power of 500 mW which is used as a baseline value that is to be optimized. The PP is connected to a MZM-based phase modulator to broaden the pump light spectrum that is a widely used technique in FOPAs to raise stimulated Brillouin scattering (SBS) threshold power in HNLF [22]. A combination of four different frequencies sinusoidal oscillations was fed to the phase

modulator electrical signal input. Frequencies of sinusoidal waves were taken from the previous research on FOPA and these are: 180, 420, 1087, and 2133 MHz [57]. A polarization controller is placed after the phase modulator to adjust the *PP* optical radiation state of polarization (SOP) to match with the WDM signals' SOP. After the polarizer, there is an isolator to prevent reflected signals from entering the pump laser. Two WDM couplers are connected to the HNLF (see Figure 1). One at the input of HNLF to combine *PP* generated pump radiation with WDM signals. The other one is connected to the HNLF output to add the backward propagating (in respect to *PP*) Raman pump (*RP*) radiation. *RP* is a CW laser with an output power of 500 mW. The *RP* frequency was set up in such a way to achieve maximum Raman gain at *PP* frequency. Isolator at the output of *RP* is for the same reason as previously mentioned—to stop reflected signals from entering the laser. WDM couplers simultaneously operate also as filters to filter out *PP* and *RP* optical radiation after propagation through the HNLF.

HNLF length used in the parametric amplifier is mainly determined by two aspects. On the one hand, HNLF length should be as short as possible to reduce dispersion induced phase mismatch between pump and signals. On the other hand, longer HNLF reduces the required pump laser power. Here we used a 1 km long HNLF fiber with zero chromatic dispersion at 1553 nm, dispersion slope of 0.016 ps/nm²/km, nonlinearity coefficient of 15.0 W⁻¹ km⁻¹, Raman Constant of 0.18, and attenuation coefficient 0.96 dB/km at 1550 nm reference wavelength. These parameters are taken from a commercial HNLF.

After the RA-FOPA amplifier section, there is an optical filter with a Gaussian type transfer function with a 3-dB bandwidth of 15 nm. It is used to filter out the idler components generated from the FWM process that are located in the L band (1565–1625 nm). The receiver section consists of a 16-channel optical power splitter. The insertion loss of this splitter is 13.5 dB at a system operation band. Subsequently, each channel is filtered using an optical Gaussian type filter with a 3-dB bandwidth of 0.25 nm. After filtering follows PIN photodiode that performs optical to electrical signal conversion. Receiver sensitivity is -21.5 dBm to provide a bit error ratio (BER) of 1×10^{-9} . The sensitivity of the PIN photodiode is indicated at sensitivity reference error probability BER = 1×10^{-12} . Electrical signals were filtered using a low pass Bessel type filter to reduce receiver induced noises. Eye diagrams were used to determine received signals BER and the studied WDM system performance was determined by the worst channel BER. A commonly used criterion for digital optical receivers requires the BER value to be below the threshold of 1×10^{-9} [10].

3. Results

Two types of fiber were used for the transmission line to generate an input signal for the preamplifier, namely 150 km of standard SMF and NZ-DSF. It was found that there was no appreciable difference in preamplifier performance when using either fiber. Further results are shown for the case of NZ-DSF.

It is also known that four-wave mixing efficiency is greatly affected by the relative polarization of signal and pump waves. This requires some form of polarization tracking or a polarization-insensitive scheme. As that is beyond the scope of this article, it was assumed that the signal and pump are co-polarized.

Due to the gain curve being dependent on pump power, both in terms of its peak gain and shape, channel placement on the spectral grid was adjusted to achieve a similar gain for the outermost channels. An increase in pump power shifts the peak gain point further away from the pump. To achieve maximally uniform output power, channels were not centered around peak gain but located slightly closer to the pump frequency. This is due to a steeper gain curve on the side further away from the pump.

Since RA-FOPA performance depends on a quite complex interaction between different nonlinear effects, it is necessary to find what *PP* and *RP* parameters should be chosen to achieve necessary gain characteristics. In this case, we have an optical signal that is composed of 16 WDM channels and per channel power -40 dBm. The main objective is

to amplify all the 16 channels (total bandwidth of 11.6 nm) evenly (ideally constant gain across all channels) so the system's worst channel BER is no worse than 1×10^{-9} .

First of all, it was necessary to empirically find out necessary *PP* and *RP* frequencies and pump powers. This was done by consecutively switching off the *RP* and *PP* at that time changing the remaining pump laser frequency and power to find a combination that gives the lowest channel to channel power difference and all the channel BER is no higher than 1×10^{-9} . It was found that the most uniform WDM channel amplification for RA-FOPA is when combining 192.918 THz and 440 mW output power *PP* and 206.13 THz and 500 mW output power *RP*.

RA-FOPA gain in the 194–200 THz frequency range is presented in Figure 2. Gain is calculated as a difference between amplified signal and signal without amplification or so-called on-off gain. Using the same parameters as RA-FOPA, the individual FOPA, and Raman amplifier gain curves, and the sum of their respective gain are shown. Raman amplifier gain is relatively low because the *RP* frequency was selected so that maximum gain matches with the *PP* frequency. Compared to the sum of Raman and FOPA gain, RA-FOPA gain is significantly larger. This confirms that the RA-FOPA amplification process is not just a sum of both amplifier gains. RA-FOPA gain enhancement in the 16 channel WDM system band is on average 8.2 dB higher than the gain sum of Raman and FOPA. The main reason for this is the indirect Raman amplification of the signal through the parametric process. The central part of the gain curve (two vertical dashed lines) where the WDM channels are located is also more even. If compared to the papers authored by other researchers, our RA-FOPA model gain enhancement is comparable to these results (6.4 dB [47] up to 10 dB [44]) for similar total pump powers (~ 1 W).

The shape of the FOPA and RA-FOPA gain curves is determined by the FWM effect. As the frequency difference between pump and signals increases, the phase-matching condition is no longer completely satisfied so the parametric gain rapidly decreases and starts to oscillate within a small range [58,59]. The average gain for the 16 channel WDM system in the case of RA-FOPA was 34.7 dB and the difference between the lowest and highest gain was 1.9 dB.

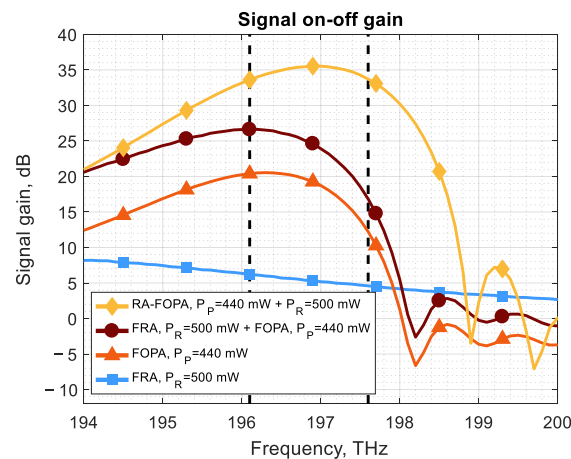


Figure 2. Signal on-off gain curves in the 194–200 THz frequency band for different amplifier combinations. The two vertical black dashed lines represent the frequency band in which all the 16 WDM channels are located.

The proposed RA-FOPA setup was also compared to single pump FOPA operating as a preamplifier in the same transmission system model. The simulation scheme with FOPA as preamplifier is the same as the previously described RA-FOPA setup (see Figure 1) without the second WDM coupler at the HNLf output and the *RP* laser. Two options were explored to reach the same peak gain as RA-FOPA. Option one—*PP* laser frequency is the same as for RA-FOPA and power is increased. Option two—*PP* laser frequency is optimized for maximum peak gain at minimum *PP* power. Accordingly, the *PP* laser wavelength

and power were 1553.99 nm, 682 mW, and 1554.10 nm, 660 mW for each case. The corresponding gain curves are shown in Figure 3. While the total pump power in the case of RA-FOPA is higher, the single pump laser case requires a more powerful light source than each individual pump laser (P_P at 440 mW and P_R at 500 mW) used in the proposed RA-FOPA configuration.

From Figure 3 it can be seen that for RA-FOPA the 3 dB gain bandwidth is 0.02 THz wider than in the case of FOPA at 682 mW and 0.20 THz wider than the optimized FOPA at 660 mW, which may be partially explained by direct signal amplification via the Raman pump.

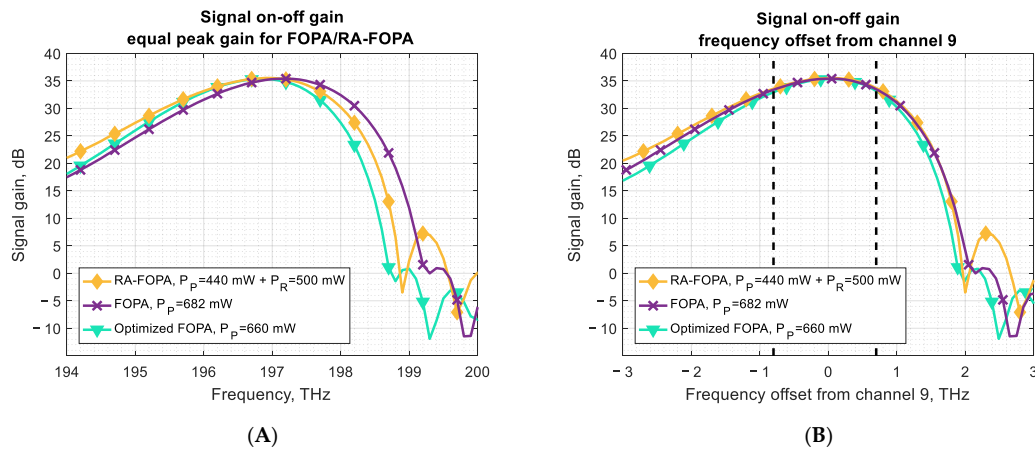


Figure 3. Fiber optical parametric amplifiers (FOPA) (violet line, crosses), optimized FOPA (cyan line, triangles) and RA-FOPA (yellow line, diamonds) signal on-off gain curves with the horizontal axis set to the (A) frequency band from 194 up to 200 THz (1498.96–1545.32 nm); (B) frequency offset from channel 9 with two vertical black dashed lines representing the frequency band in which all 16 WDM channels are located.

A comparison of received optical power among all the 16 WDM channels after 1:16 power splitter with an insertion loss of 13.5 dB is given in Figure 4. A similar shape can be seen, but RA-FOPA results in more uniform output power. Figure 4B shows a closer view of the three amplifier variants.

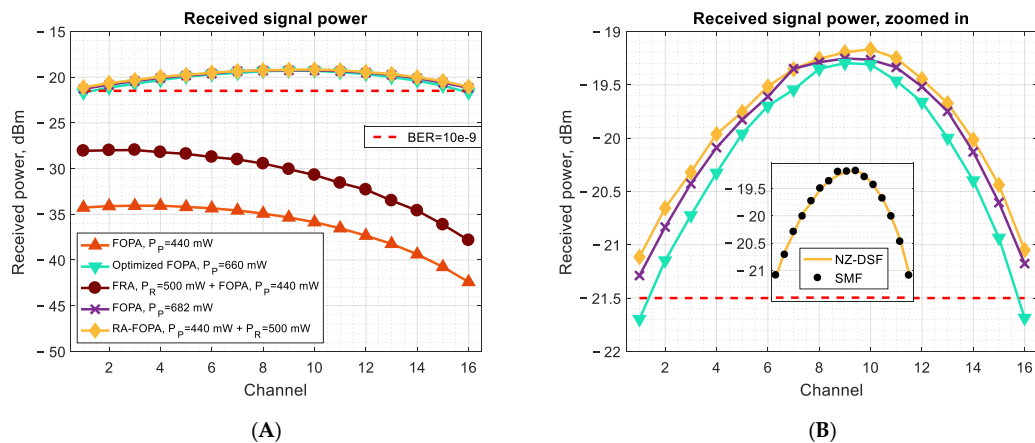


Figure 4. (A) Received signal power distribution of all 16 WDM channels in the case of RA-FOPA and FOPA combinations. Signal power obtained as the sum of the individual Fiber Raman amplifier (FRA) and FOPA gain is also shown. (B) Zoomed in view of (A) only showing the RA-FOPA, FOPA, and optimized FOPA. Inset in (B) shows similarities in received power when using SMF and NZ-DSF fibers for transmission.

From Figure 5 it can be seen that at the signal power shown in Figure 4, FOPA has a BER comparable to RA-FOPA. However, the 16th channel shows worse performance due to the steeper gain curve of FOPA resulting in a lower channel power.

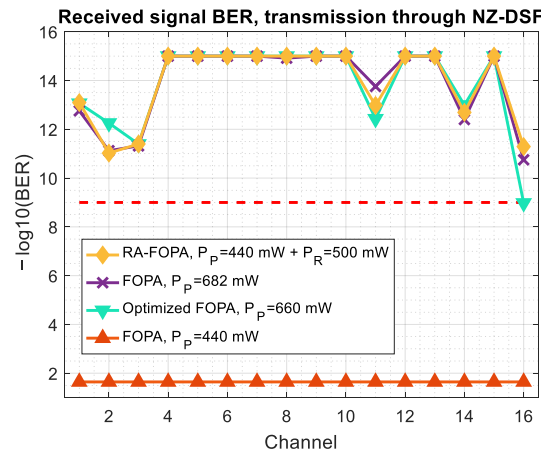


Figure 5. Bit error ratio (BER) distribution between all 16 WDM channels in the case of FOPA and RA-FOPA. Results are limited to BER of 1×10^{-15} threshold for better visibility. BER evaluation accuracy is up to \pm one order of magnitude. Red dashed line is BER = 10^{-9} threshold.

We have calculated all 16 WDM channel OSNRs using received signal Quality factor (Q), where $BER = \frac{1}{2}erfc\left(\frac{Q}{\sqrt{2}}\right)$ for on-off keying signals. Received signal quality factor relation to OSNR is given in the following equation:

$$Q_{linear} = 10 \cdot \log_{10} \left(2 \cdot 10^{OSNR_{dB}/10} \cdot \frac{B_n}{R_b} \right),$$

where B_n is noise bandwidth and R_b is symbol rate [60]. Before the OSNR calculation, all the received signals were equalized with regard to power (-21.7 dBm) since the simulation model calculates Q factor directly proportionally to power. This was done in order to make a more realistic comparison of three amplifiers (RA-FOPA, FOPA, and optimized FOPA) regarding received signal noise rather the absolute power level. As seen in Figure 6, the received signal OSNR (calculated at a resolution of 0.01 THz) in the case of RA-FOPA is comparable to both FOPA configurations. Accordingly the mean and standard deviation of the OSNR for the three configurations (excluding the outermost channels): RA-FOPA 18.57 ± 0.53 dB, FOPA 18.52 ± 0.45 dB, and finally the peak-gain optimized FOPA 18.59 ± 0.61 dB. This shows that after equalization of received signal power all three amplifiers produce a similar level of noise. It should be noted that both single pump FOPAs have significantly higher parametric pump lasers, to achieve the same output power and OSNR levels.

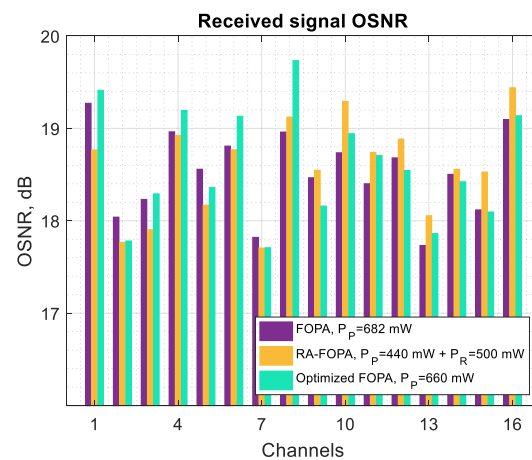


Figure 6. All 16 WDM channel optical signal to noise ratio (OSNR) distribution in the case of FOPA, RA-FOPA and peak-gain-optimized FOPA. OSNR values are calculated from received signal BER at equalized received signal power level (-21.7 dBm).

4. Discussion

In this article, RA-FOPA amplifier performance in a multichannel WDM system was studied and compared to single pump FOPA using computer simulations. This includes Raman and parametric combined amplification process analysis and its application in 16 channel 40 Gbps WDM system. The operational conditions were uniform channel amplification while keeping received signal BER levels below the 1×10^{-9} threshold.

Results showed that RA-FOPA gain is more even and its -3 dB gain bandwidth is 0.02 THz wider than in the case of FOPA at 682 mW and 0.20 THz wider than the peak-gain optimized FOPA at 660 mW, which may be explained by direct signal amplification via the Raman pump. However, the output optical power difference among all the 16 WDM channels was very similar apart from the 16th channel for the optimized FOPA not reaching the 1×10^{-9} BER threshold.

The amplified signal OSNR in the case of RA-FOPA was similar to the other two FOPA configurations (~ 18.6 dB). Therefore single pump FOPA can be optimized regarding output signal quality but it requires significantly higher parametric pump power (440 mW versus 682 mW).

While the pump power ($PP = 682$ mW) in the case of single pump FOPA is lower by 38% compared to the total pump power ($PP = 440$ mW and $RP = 500$ mW) in the proposed RA-FOPA configuration, the required FOPA pump power is more than 36% higher than each individual RA-FOPA pump laser. Higher single pump power comes with implementation concerns, such as heat dissipation, efficiency, and SBS limitations on launch power.

From results acquired in this research, it can be concluded that combined Raman-FOPA has considerable benefits to WDM system applications. Moreover, this solution could be used to substantially improve the performance of existing FOPA amplifiers.

Author Contributions: Conceptualization: A.S., K.Z., J.P. and V.B.; methodology: A.S., K.Z. and S.S.; software: K.Z., L.G. and D.R.; validation: A.S., K.Z., L.G., D.R., S.S. and J.P.; formal analysis: K.Z., S.S. and J.P.; investigation: K.Z., S.S. and J.P.; resources: J.P. and V.B.; data curation: A.S. and K.Z.; writing—original draft preparation A.S. and K.Z.; writing—review and editing: A.S. and S.S.; visualization: K.Z. and S.S.; supervision: J.P. and V.B.; project administration: J.P. and V.B.; funding acquisition: A.S. and V.B. All authors have read and agreed to the published version of the manuscript.

Funding: This work has been supported by the European Regional Development Fund within the Activity 1.1.1.2 “Post-doctoral Research Aid” of the Specific Aid Objective 1.1.1 “To increase the research and innovative capacity of scientific institutions of Latvia and the ability to attract external financing, investing in human resources and infrastructure” of the Operational Programme “Growth and Employment” (No. 1.1.1.2/VIAA/1/16/151).

Conflicts of Interest: The authors declare no conflict of interest.

References

1. Cisco. *Cisco Visual Networking Index: Global Mobile Data Traffic Forecast Update, 2017–2022*; Cisco: San Jose, CA, USA, 2019.
2. Ericsson. *Mobility Report November 2018*; Ericsson: Stockholm, Sweden, 2018; p. 32.
3. Essiambre, R.-J.; Kramer, G.; Winzer, P.J.; Foschini, G.J.; Goebel, B. Capacity Limits of Optical Fiber Networks. *J. Lightwave Technol.* **2010**, *28*, 662–701. [\[CrossRef\]](#)
4. Saxena, A.; Dastoor, Y.; Prajapati, P.R. Flat Gain on C-Band Using Raman-EDFA Hybrid Optical Amplifier for DWDM System. *J. Switch. Hub.* **2018**, *3*, 2.
5. Kaur, G.; Kaur, G.; Sharma, S. Multisection optical parametric–Raman hybrid amplifier for terabit+ WDM systems. *J. Mod. Opt.* **2015**, *63*, 819–825. [\[CrossRef\]](#)
6. Obaid, H.M.; Shahid, H. Performance evaluation of hybrid optical amplifiers for a 100×10 Gbps DWDM system with ultrasmall channel spacing. *Optik* **2020**, *200*. [\[CrossRef\]](#)
7. Bobrovs, V.; Olonkins, S.; Spolitis, S.; Porins, J.; Ivanovs, G.; Ivanovs, J.P.A.G. Evaluation of Parametric and Hybrid Amplifier Applications in WDM Transmission Systems. In *Optical Fiber and Wireless Communications*; IntechOpen: London, UK, 2017.
8. Kaur, G.; Sharma, S. New dispersion-compensated Raman-amplifier cascade with a single-pump parametric amplifier for dense wavelength-division multiplexing. *Ukr. J. Phys. Opt.* **2020**, *21*, 35–46. [\[CrossRef\]](#)

9. Fukuchi, K. Wideband and ultra-dense WDM transmission technologies toward over 10-Tb/s capacity. *Opt. Fiber Commun. Conf. Exhib.* **2003**, *5*. [[CrossRef](#)]
10. Agrawal, G.P. *Fiber-Optic Communication Systems; Wiley Series in Microwave and Optical Engineering*, 4th ed.; Wiley: New York, NY, USA, 2010; ISBN 978-0-470-50511-3.
11. Olonkins, S.; Spolitis, S.; Lyashuk, I.; Bobrovs, V. Cost effective WDM-AON with multicarrier source based on dual-pump FOPA. In Proceedings of the 2014 6th International Congress on Ultra Modern Telecommunications and Control Systems and Workshops (ICUMT), St. Petersburg, Russia, 6–8 October 2014; pp. 23–28.
12. Zyskind, J.; Bolshtyansky, M. EDFAs, Raman Amplifiers and Hybrid Raman/EDFAs. In *Optically Amplified WDM Networks*; Elsevier BV: Berlin, Germany, 2011; pp. 83–116.
13. Emami, S.D.; Hajireza, P.; Abd-Rahman, F.; Abdul-Rashid, H.A.; Ahmad, H.; Harun, S.W. Wide-band hybrid amplifier operating in s-band region. *Prog. Electromagn. Res.* **2010**, *102*, 301–313. [[CrossRef](#)]
14. Yam, S.-H.; Kim, J. Ground state absorption in thulium-doped fiber amplifier: Experiment and modeling. *IEEE J. Sel. Top. Quantum Electron.* **2006**, *12*, 797–803. [[CrossRef](#)]
15. Peterka, P.; Faure, B.; Blanc, W.; Karásek, M.; Dussardier, B. Theoretical modelling of S-band thulium-doped silica fibre amplifiers. *Opt. Quantum Electron.* **2004**, *36*, 201–212. [[CrossRef](#)]
16. Kozak, M.; Caspary, R.; Kowalsky, W. Thulium-doped fiber amplifier for the S-band. *Proc. 2004 6th Int. Conf. Trans. Opt. Network.* **2004**, *2*, 51–54.
17. Andrianov, A.; Anashkina, E.A. Single-mode silica microsphere Raman laser tunable in the U-band and beyond. *Results Phys.* **2020**, *17*. [[CrossRef](#)]
18. Raman Amplifiers for Telecommunications; Islam, M.N. *Springer Series in Optical Sciences*; Springer: New York, NY, USA, 2004; ISBN 978-0-387-00751-9.
19. Singh, K.; Kaur, P.; Devra, S.; Kaur, G. Evaluation of gain spectrum of dual/triple pumped fiber Raman amplifier (FRA) by optimizing its pumping parameters in the scenario of dense wavelength division multiplexed (DWDM) systems. *Optik* **2019**, *176*, 246–253. [[CrossRef](#)]
20. Nicholson, J. Dispersion compensating Raman amplifiers with pump reflectors for increased efficiency. *J. Light. Technol.* **2003**, *21*, 1758–1762. [[CrossRef](#)]
21. Anashkina, E.A.; Andrianov, A.V.; Dorofeev, V.; Kim, A.; Koltashev, V.; Leuchs, G.; Motorin, S.; Muravyev, S.; Plekhovich, A. Development of infrared fiber lasers at 1555 nm and at 2800 nm based on Er-doped zinc-tellurite glass fiber. *J. Non-Cryst. Solids* **2019**, *525*. [[CrossRef](#)]
22. Marhic, M.E. (Ed.) *Fiber Optical Parametric Amplifiers, Oscillators and Related Devices*; Cambridge University Press: Cambridge, UK, 2007.
23. Hk, E.K.; Fm, M.; Tm, B. Optimizing of Raman Gain and Bandwidth for Dual Pump Fiber Optical Parametric Amplifiers Based on Four-Wave Mixing. *J. Telecommun. Syst. Manag.* **2018**, *7*, 1–4. [[CrossRef](#)]
24. Othman, N.; Tay, K.G.; Shah, N.S.M.; Talib, R.; Pakarzadeh, H.; Cholan, N.A. Saturation behavior of a one-pump fiber optical parametric amplifier in the presence of the fourth-order dispersion coefficient and dispersion fluctuation. *Chin. Opt. Lett.* **2019**, *17*. [[CrossRef](#)]
25. Othman, N.; Tay, K.G.; Talib, R.; Cholan, N.A.; Shah, N.S.M.; Pakarzadeh, H. Saturation Behavior of Fiber Optical Parametric Amplifier in Presence of Dispersion Fluctuations. In Proceedings of the 2018 IEEE 7th International Conference on Photonics (ICP), Kuah, Malaysia, 9–11 April 2018; pp. 1–3.
26. Boyd, R.W. *Nonlinear Optics*; Elsevier Science: Saint Louis, MO, USA, 2014; ISBN 978-1-4832-8823-9.
27. Inoue, K.; Mukai, T. Signal wavelength dependence of gain saturation in a fiber optical parametric amplifier. *Opt. Lett.* **2001**, *26*, 10–12. [[CrossRef](#)]
28. Torounidis, T.; Sunnerud, H.; Hedekvist, P.; Andrekson, P. Amplification of WDM signals in fiber-based optical parametric amplifiers. *IEEE Photon. Technol. Lett.* **2003**, *15*, 1061–1063. [[CrossRef](#)]
29. Deng, Y.; Yu, C.; Yuan, J.; Sang, X.; Li, W. Raman-induced limitation of gain flatness in broadband fiber-optical parametric amplifier. *Opt. Eng.* **2012**, *51*, 045003. [[CrossRef](#)]
30. Torounidis, T.; Andrekson, P.; Olsson, B.-E. Fiber-optical parametric amplifier with 70-dB gain. *IEEE Photon. Technol. Lett.* **2006**, *18*, 1194–1196. [[CrossRef](#)]
31. Ho, M.-C.; Uesaka, K.; Marhic, M.; Akasaka, Y.; Kazovsky, L. 200-nm-bandwidth fiber optical amplifier combining parametric and Raman gain. *J. Light. Technol.* **2001**, *19*, 977–981. [[CrossRef](#)]
32. Szabö, Á.D.; Ribeiro, V.; Gordienko, V.; Ferreira, F.; Gaur, C.; Doran, N. Verification of Signal-to-Crosstalk Measurements for WDM Fiber Optical Parametric Amplifiers. In Proceedings of the Conference on Lasers and Electro-Optics, San Jose, CA, USA, 10–15 May 2020; p. JTu2E.1.
33. Gordienko, V.; Ferreira, F.M.; Ribeiro, V.; Doran, N. Suppression of Nonlinear Crosstalk in a Polarization Insensitive FOPA by Mid-stage Idler Removal. In Proceedings of the Optical Fiber Communication Conference (OFC), San Diego, CA, USA, 3–7 March 2019; p. M4C.4.
34. Krastev, K.; Rothman, J.K.K.J.R. Crosstalk in fiber parametric amplifier. In Proceedings of the Proceedings 27th European Conference on Optical Communication (Cat. No.01TH8551), Amsterdam, The Netherlands, 30 September–4 October 2001; Volume 3, pp. 378–379.

35. Stephens, M.F.C.; Tan, M.; Gordienko, V.; Harper, P.; Doran, N.J. In-line and cascaded DWDM transmission using a 15dB net-gain polarization-insensitive fiber optical parametric amplifier. *Opt. Express* **2017**, *25*, 24312–24325. [[CrossRef](#)]
36. Gordienko, V.; Ferreira, F.; Laperle, C.; O’Sullivan, M.; Gaur, C.B.; Roberts, K.; Doran, N. Noise Figure Evaluation of Polarization-insensitive Single-pump Fiber Optical Parametric Amplifiers. In Proceedings of the Optical Fiber Communication Conference (OFC), San Diego, CA, USA, 8–12 March 2020; p. W4B.4.
37. Stephens, M.F.C.; Gordienko, V.; Doran, N.J. Reduced Crosstalk, Polarization Insensitive Fiber Optical Parametric Amplifier (PI FOPA) for WDM Applications. In Proceedings of the Optical Fiber Communication Conference Postdeadline Papers, San Diego, CA, USA, 11–15 March 2018; p. W3D.4.
38. Yeo, K.; Adikan, F.M.; Mokhtar, M.; Hitam, S.; Mahdi, M. Gain smoothening filter in two-segment fiber-optical parametric amplifier. *Opt. Commun.* **2013**, *286*, 353–356. [[CrossRef](#)]
39. Yeo, K.S.; Adikan, F.R.M.; Mokhtar, M.; Hitam, S.; Mahdi, M.A. Fiber optical parametric amplifier with double-pass pump configuration. *Opt. Express* **2013**, *21*, 31623–31631. [[CrossRef](#)]
40. Lei, G.K.P.; Marhic, M.E. Amplification of DWDM channels at 128 Tb/s in a bidirectional fiber optical parametric amplifier. *Opt. Express* **2014**, *22*. [[CrossRef](#)]
41. Guo, X.; Fu, X.; Shu, C. Gain saturation in a Raman-assisted fiber optical parametric amplifier. *Opt. Lett.* **2013**, *38*, 4405–4408. [[CrossRef](#)]
42. Guo, X.; Fu, X.; Shu, C. Gain-saturated spectral characteristics in a Raman-assisted fiber optical parametric amplifier. *Opt. Lett.* **2014**, *39*, 3658–3661. [[CrossRef](#)]
43. Kaur, G.; Sharma, S.; Kaur, G. Novel Raman Parametric Hybrid L-Band Amplifier with Four-Wave Mixing Suppressed Pump for Terabits Dense Wavelength Division Multiplexed Systems. *Adv. Opt. Technol.* **2016**, *2016*, 1–8. [[CrossRef](#)]
44. Wang, S.H.; Wai, P.K.A. Gain Enhancement in Hybrid Fiber Raman/Parametric Amplifiers. In Proceedings of the Conference on Lasers and Electro-Optics, San Jose, CA, USA, 16–21 May 2010; p. 56.
45. De Matos, C.J.S.; Chestnut, D.A.; Reeves-Hall, P.C.; Taylor, J.R. Continuous-wave-pumped Raman-assisted fiber optical parametric amplifier and wavelength converter in conventional dispersion-shifted fiber. *Opt. Lett.* **2001**, *26*, 1583–1585. [[CrossRef](#)]
46. Chestnut, D.A.; De Matos, C.J.S.; Taylor, J.R. Raman-assisted fiber optical parametric amplifier and wavelength converter in highly nonlinear fiber. *J. Opt. Soc. Am. B* **2002**, *19*, 1901–1904. [[CrossRef](#)]
47. Wang, S.H.; Xu, L.; Wai, P.K.A.; Tam, H.-Y. Optimization of Raman-Assisted Fiber Optical Parametric Amplifier Gain. *J. Light. Technol.* **2011**, *29*, 1172–1181. [[CrossRef](#)]
48. Wang, S.H.; Xu, L.; Wai, P.K.A.; Tam, H.-Y. 6.4-dB Small signal gain enhancement in Raman-assisted fiber optical parametric amplifiers. In Proceedings of the 2008 Conference on Lasers and Electro-Optics, San Jose, CA, USA, 4–9 May 2008; pp. 1–2.
49. Stephens, M.F.C.; Philips, I.D.; Rosa, P.; Harper, P.; Doran, N. Improved WDM performance of a fibre optical parametric amplifier using Raman-assisted pumping. *Opt. Express* **2015**, *23*, 902–911. [[CrossRef](#)]
50. Fludger, C.; Handerek, V.; Mears, R. Pump to signal RIN transfer in Raman fiber amplifiers. *J. Light. Technol.* **2001**, *19*, 1140–1148. [[CrossRef](#)]
51. Salman, M.H.; Hassan, A.H.; Yasser, H.A. Theoretical Calibration of Raman-Assisted Fiber Optical Parametric Amplifiers in Wavelength-Division Multiplexing. *IPASJ Int. J. Electron. Commun.* **2014**, *2*, 9.
52. OptSim—Photonic System Tools Synopsys Photonic Solutions. Available online: <https://www.synopsys.com/photonic-solutions/rsoft-system-design-tools/system-network-optsim.html> (accessed on 8 January 2021).
53. Laming, R.; Gnauck, A.; Giles, C.; Zervas, M.N.; Payne, D. High-sensitivity two-stage erbium-doped fiber preamplifier at 10 Gb/s. *IEEE Photon. Technol. Lett.* **1992**, *4*, 1348–1350. [[CrossRef](#)]
54. Liang, Y.; Li, J.; Chui, P.; Wong, K. High-Sensitivity Optical Preamplifier for WDM Systems Using an Optical Parametric Amplifier. *IEEE Photon. Technol. Lett.* **2009**, *21*, 1562–1564. [[CrossRef](#)]
55. Hansryd, J.; Andrekson, P. Broad-band continuous-wave-pumped fiber optical parametric amplifier with 49-dB gain and wavelength-conversion efficiency. *IEEE Photon. Technol. Lett.* **2001**, *13*, 194–196. [[CrossRef](#)]
56. Olonkins, S.; Supe, A.; Bobrovs, V.; Prigunovs, D. Comparison of Single-pump FOPA and Raman Assisted FOPA Performance in a 16 Channel DWDM Transmission System. In Proceedings of the 2019 Photonics & Electromagnetics Research Symposium-Fall (PIERS-Fall), Xiamen, China, 17–20 December 2019; pp. 723–727.
57. Olonkins, S.; Bobrovs, V.; Ivanovs, G. Investigation of Fiber Optical Parametric Amplifier Performance in DWDM Transmission Systems. *Elektron. Elektrotech.* **2014**, *20*, 88–91. [[CrossRef](#)]
58. Silva, N.A.; Muga, N.J.; Pinto, A.N. Effective Nonlinear Parameter Measurement Using FWM in Optical Fibers in a Low Power Regime. *IEEE J. Quantum Electron.* **2009**, *46*, 285–291. [[CrossRef](#)]
59. Supe, A.; Fernandes, G.; Muga, N.; Pinto, A.; Ferreira, M. Experimental Characterization of a Highly Nonlinear Fiber. In *8th Iberoamerican Optics Meeting and 11th Latin American Meeting on Optics, Lasers, and Applications*; Martins Costa, M.F.P.C., Ed.; International Society for Optics and Photonics: Porto, Portugal, 18 November 2013; p. 87854D.
60. Liu, X.; Luan, H.; Dai, B.; Lan, B. Influence of fiber link impairments to Eb/No estimation in CO-OFDM systems with QPSK mapping. *Optik* **2013**, *124*, 1977–1981. [[CrossRef](#)]